

## Photochemical Mineralization of Europium, Titanium, and Iron Oxyhydroxide Nanoparticles in the Ferritin Protein Cage

Michael T. Klem,<sup>†,‡</sup> Jesse Mosolf,<sup>†,‡</sup> Mark Young,<sup>\*,‡,§</sup> and Trevor Douglas<sup>\*,†,‡</sup>

Department of Chemistry & Biochemistry, Department of Plant Sciences, and Center for BioInspired Nanomaterials, Montana State University, Bozeman, Montana 59717

Received September 4, 2007

The Fe storage protein ferritin was used as a size-constrained reaction vessel for the photoreduction and reoxidation of complexed Eu, Fe, and Ti precursors for the formation of oxyhydroxide nanoparticles. The resultant materials were characterized by dynamic light scattering, gel electrophoresis, UV–vis spectroscopy, and transmission electron microscopy. The photoreduction and reoxidation process is inspired by biological sequestration mechanisms observed in some marine siderophore systems.

Biomimetic approaches to materials chemistry provide new avenues for the synthesis and assembly of nanomaterials.<sup>1–6</sup> There is growing interest in materials chemistry to take advantage of the physical and chemical properties of biomolecules for development of the next generation of nano-scale materials.<sup>7</sup> Bioinspired approaches to materials synthesis have utilized well-defined protein architectures,<sup>8–13</sup>

macromolecular templates,<sup>14</sup> and evolved molecular interactions<sup>15</sup> to exert synthetic control over crystal morphology, phase, and orientation. In particular, protein cage architectures having high symmetry have been shown to act as constrained reaction environments for the synthesis and encapsulation of inorganic and organic nanomaterials.<sup>5,8,10–12,16</sup>

Using a biomimetic approach to materials synthesis, we have developed a photochemical approach to generate transient reduced metal species from an extremely stable pool of chelated high-oxidation-state metal ions. The efficacy of this approach was demonstrated by the spatially selective mineralization of the spherical Fe storage protein cage ferritin, which resulted in the formation of a stable metal oxyhydroxide nanoparticles encapsulated within the protein cage as potential precursors to other oxide materials.

Ferritins consist of 24 protein subunits that self-assemble into a cage-like architecture with an exterior diameter of 12 nm and an interior diameter of 8 nm in which a hydrated ferric oxide/phosphate is mineralized. Ferritins have evolved to sequester Fe *in vivo*, but the protein has been used as a template in synthetic reactions with various metal ions, which results in the formation of inorganic nanoparticles constrained exclusively within the protein cage architecture. Materials such as Fe<sub>3</sub>O<sub>4</sub>,<sup>13,17–21</sup> Co<sub>3</sub>O<sub>4</sub>,<sup>8,22</sup> Mn<sub>3</sub>O<sub>4</sub>,<sup>23–25</sup> CoPt,<sup>26</sup> Pd,<sup>27</sup>

\* To whom correspondence should be addressed. E-mail: myoung@montana.edu (M.Y.), tdouglas@chemistry.montana.edu (T.D.).

<sup>†</sup> Department of Chemistry & Biochemistry.

<sup>‡</sup> Department of Plant Sciences.

<sup>§</sup> Center for BioInspired Nanomaterials.

- (1) Lee, S. W.; Mao, C. B.; Flynn, C. E.; Belcher, A. M. *Science* **2002**, *296*, 892.
- (2) Mann, S. *Biomimetic Materials Chemistry*; VCH: New York, 1996.
- (3) Mann, S.; Archibald, D. D.; Didymus, J. M.; Douglas, T.; Heywood, B. R.; Meldrum, F. C.; Reeves, N. J. *Science* **1993**, *261*, 1286.
- (4) Naik, R. R.; Stringer, S. J.; Agarwal, G.; Jones, S. E.; Stone, M. O. *Nat. Mater.* **2002**, *1*, 169.
- (5) Uchida, M.; Klem, M. T.; Allen, M.; Suci, P.; Flenniken, M.; Gillitzer, E.; Varpness, Z.; Liepold, L. O.; Young, M.; Douglas, T. *Adv. Mater.* **2007**, *19*, 1025.
- (6) Whaley, S. R.; English, D. S.; Hu, E. L.; Barbara, P. F.; Belcher, A. M. *Nature* **2000**, *405*, 665.
- (7) Niemeyer, C. M. *Angew. Chem., Int. Ed.* **2001**, *40*, 4128.
- (8) (a) Allen, M.; Willits, D.; Young, M.; Douglas, T. *Inorg. Chem.* **2003**, *42*, 6300. (b) Klem, M. T.; Willits, D.; Young, M.; Douglas, T. *J. Am. Chem. Soc.* **2003**, *125*, 10806. (c) Hosein, H. A.; Strongin, D. R.; Allen, M.; Douglas, T. *Langmuir* **2004**, *20*, 10283.
- (9) Douglas, T.; Dickson, D. P. E.; Betteridge, S.; Charnock, J.; Garner, C. D.; Mann, S. *Science* **1995**, *269*, 54.
- (10) Douglas, T.; Strable, E.; Willits, D.; Aitouchen, A.; Libera, M.; Young, M. *Adv. Mater.* **2002**, *14*, 415.
- (11) Douglas, T.; Young, M. *Nature* **1998**, *393*, 152.
- (12) Mann, S.; Ozin, G. A. *Nature* **1996**, *382*, 313.
- (13) Meldrum, F. C.; Heywood, B. R.; Mann, S. *Science* **1992**, *257*, 522.

- (14) Shenton, W.; Douglas, T.; Young, M.; Stubbs, G.; Mann, S. *Adv. Mater.* **1999**, *11*, 253.
- (15) Allen, M.; Willits, D.; Mosolf, J.; Young, M.; Douglas, T. *Adv. Mater.* **2002**, *14*, 1562.
- (16) McMillan, R. A.; Paavola, C. D.; Howard, J.; Chan, S. L.; Zaluzec, N. J.; Trent, J. D. *Nat. Mater.* **2002**, *1*, 247.
- (17) Bulte, J. W. M.; Douglas, T.; Mann, S.; Frankel, R. B.; Moskowitz, B. M.; Brooks, R. A.; Baumgarner, C. D.; Vymazal, J.; Frank, J. A. *Invest. Radiol.* **1994**, *29*, S214.
- (18) Gider, S.; Awschalom, D. D.; Douglas, T.; Mann, S.; Chaparala, M. *Science* **1995**, *268*, 77.
- (19) Gider, S.; Awschalom, D. D.; Douglas, T.; Wong, K.; Mann, S.; Cain, G. *J. Appl. Phys.* **1996**, *79*, 5324.
- (20) Pankhurst, Q. A.; Betteridge, S.; Dickson, D. P. E.; Douglas, T.; Mann, S.; Frankel, R. B. *Hyperfine Interact.* **1994**, *91*, 847.
- (21) Wong, K. K. W.; Douglas, T.; Gider, S.; Awschalom, D. D.; Mann, S. *Chem. Mater.* **1998**, *10*, 279.
- (22) Resnick, D. A.; Gilmore, K.; Idzerda, Y. U.; Klem, M. T.; Allen, M.; Douglas, T.; Young, M.; Arenholz, E. *J. Appl. Phys.* **2006**, *99*, 08Q501.
- (23) Mackle, P.; Charnock, J. M.; Garner, C. D.; Meldrum, F. C.; Mann, S. *J. Am. Chem. Soc.* **1993**, *115*, 8471.
- (24) Mann, S. *Nature* **1991**, *349*, 285–286.

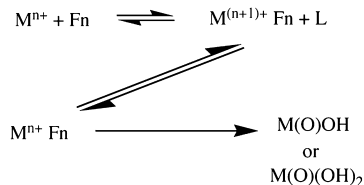


**Figure 1.** Summary of the photochemical reaction cycle of  $M(III)L$  [ $M = \text{Eu, Fe, or Ti}$  (as a IV salt);  $L = \text{citrate}$ ] and ferritin (Fn) to produce oxyhydroxides in the ferritin protein cage. The metal citrate salts are illuminated with a xenon arc lamp to reduce a small amount of the chelated metal precursor, and this subsequently undergoes a reoxidation to form a metal oxyhydroxide inside the protein cage.

$\text{Ag},^{28} \text{Cu},^{29,30} \text{CdS},^{31} \text{CdSe},^{32}$  and  $\text{ZnSe}^{33}$  have been synthesized within protein cages. The *in vitro* mineralization of ferritin is usually accomplished by a metal ion oxidative hydrolysis polymerization. Typically, a low-oxidation-state metal ion is oxidized in the presence of the protein, and the resulting higher oxidation state metal, being a much stronger Lewis acid, undergoes a hydrolytic polymerization resulting in the formation of an insoluble metal oxyhydroxide material, which precipitates from solution inside the cage structure of ferritin. Mineralization of ferritin using high-oxidation-state metal ion starting materials has not been successful.

Here we report the photoinduced mineralization of mammalian ferritin using high-oxidation-state metal ions as starting materials. Using this methodology, we have successfully mineralized ferritin cages with iron, titanium, and europium oxyhydroxide nanoparticles in a spatially selective manner encapsulated within the protein cages. The resulting materials are uniform and monodispersed and represent a new synthetic approach to the formation of transition-metal oxide materials in the nanoscale size regime.

This photochemical reduction closely mimics the photochemical reduction of iron(III) and the subsequent release of iron(II) observed in marine siderophores that have a citrate backbone (Figure 1).<sup>34,35</sup> Briefly outlined, the ferritin protein cages were incubated in a 12 mM metal citrate solutions [ $\text{metal (M)} = \text{Eu(III), Fe(III), or Ti(IV)}$ ], corresponding to a theoretical loading of 1000 M atoms per ferritin (Supporting Information), and illuminated with a xenon arc lamp (175 W, Lambda-LS, Sutter Instruments, 320–700 nm), to approximate solar irradiation, over a 2 h period (for complete reaction conditions, see the Supporting Information) of the high-oxidation-state metal precursor is critical because of the free high-oxidation-state metal ions in solution promotes bulk

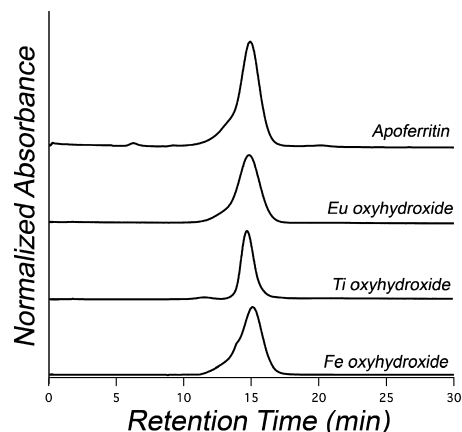


**Figure 2.** Size-exclusion chromatography profile for empty (apo)ferritin and ferritin containing the europium, titanium, or iron oxyhydroxides indicating that the mineralization process is occurring on the interior surface of the protein cage (absorbance monitored at 280 nm).

precipitation. Illumination resulted in the photoreduction of the high-oxidation-state metal citrate salt to produce transient low-oxidation-state metal ions that in the presence of air underwent reoxidation to form a metal oxyhydroxide inside the protein cages after dissociation of the citrate. In contrast, control reactions using low-oxidation-state metal ion in the absence of citrate resulted in bulk precipitation when illuminated. When this approach was taken using iron(III) citrate, in air, photolysis resulted in the mineralization of an  $\text{Fe(O)OH}$  particle within the protein cage. However, under  $\text{N}_2$ , no mineralization was observed, and under these conditions,  $\text{Fe(II)}$  was easily detected by trapping it as the  $\text{Fe(phen)}_3^{2+}$  complex. This is in agreement with the formation of  $\text{Fe(II)}$  by the photolysis reaction. The presence of  $\text{O}_2$  resulted in the reoxidation to  $\text{Fe(III)}$ , which in the presence of the apoferritin cage resulted in the spatially selective mineralization of  $\text{Fe(O)OH}$ .

A similar approach was utilized for the selective mineralization of  $\text{Eu(O)OH}$  nanoparticles within the ferritin protein cage.  $\text{Eu(II)}$  is susceptible to oxidation to  $\text{Eu(III)}$ , and attempts to use  $\text{Eu(II)}$  as a precursor for oxidative mineralization of apoferritin resulted in the spontaneous bulk precipitation of  $\text{Eu(O)OH}$ . However, when europium(III) citrate was photolyzed, in the presence of apoferritin, no bulk precipitation was observed and the reaction remained clear and homogeneous. In contrast, photolysis of europium(III) citrate in apoferritin-free control reactions resulted in the formation of a white precipitate.

The photolysis of titanium(IV) citrate in the presence of ferritin resulted in the formation of a clear homogeneous solution. In contrast, when the reaction was carried out in the absence of protein, a bulk white precipitate was observed. The reaction appears to proceed by a reduction of the high-oxidation-state transition metal through excitation of a charge-transfer transition in the  $\text{Ti(IV)}$  case. This could be demonstrated in the case of the  $\text{Ti}$  reaction when photolysis was performed under  $\text{N}_2$ , thus preventing the possibility of reoxidation of  $\text{Ti(III)}$  formed during the photolysis. Under these conditions, the characteristic purple color for the  $d^1 \text{Ti(III)}$  species could be observed within minutes of initiating photolysis.

- (25) Meldrum, F. C.; Douglas, T.; Levi, S.; Arosio, P.; Mann, S. *J. Inorg. Biochem.* **1995**, *58*, 59.  
 (26) Klem, M. T.; Willits, D. A.; Solis, D. J.; Belcher, A.; Young, M.; Douglas, T. *Adv. Funct. Mater.* **2005**, *15*, 1489.  
 (27) Ueno, T.; Suzuki, M.; Goto, T.; Matsumoto, T.; Nagayama, K.; Watanabe, Y. *Angew. Chem., Int. Ed.* **2004**, *43*, 2527.  
 (28) Kramer, R. M.; Li, C.; Carter, D. C.; Stone, M. O.; Naik, R. R. *J. Am. Chem. Soc.* **2004**, *126*, 13282.  
 (29) Ensign, D.; Young, M.; Douglas, T. *Inorg. Chem.* **2004**, *43*, 3441.  
 (30) Galvez, N.; Sanchez, P.; Dominguez-Vera, J. M. *Dalton Trans.* **2005**, 2492.  
 (31) Wong, K. K. W.; Mann, S. *Adv. Mater.* **1996**, *8*, 928.  
 (32) Yamashita, I.; Hayashi, J.; Hara, M. *Chem. Lett.* **2004**, *33*, 1158.  
 (33) Iwahori, K.; Yoshizawa, K.; Muraoka, M.; Yamashita, I. *Inorg. Chem.* **2005**, *44*, 6393.  
 (34) Barbeau, K. *Photochem. Photobiol.* **2006**, *82*, 1505.  
 (35) Barbeau, K.; Rue, E. L.; Trick, C. G.; Bruland, K. T.; Butler, A. *Limnol. Oceanogr.* **2003**, *48*, 1069.

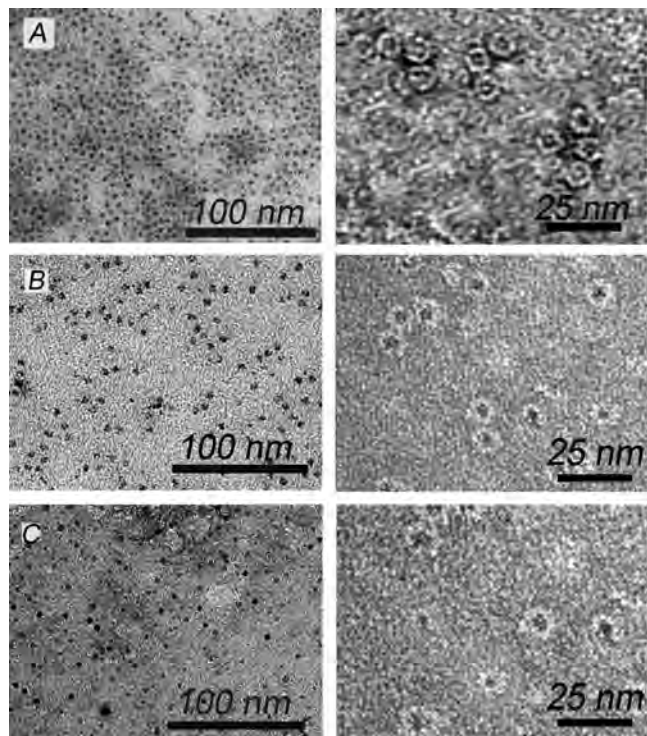


**Figure 3.** TEM micrographs of unstained (left) and uranyl acetate stained (right) photomineralized (A) europium oxyhydroxide, (B) iron oxyhydroxide, and (C) titanium oxyhydroxide nanoparticles in the protein cage ferritin. The white “halo” surrounding each particle in the stained images are due to the protein cage ferritin.

The products of all of the photolysis reactions were investigated using dynamic light scattering and found to have the same size distribution as the original protein cage starting materials ( $12 \pm 1$  nm diameter; Supporting Information). This indicates the high degree of spatial selectivity with which the mineralization reaction occurs and suggests that the inorganic nanomaterials are entrapped within the confines of the ferritin protein cage. The reaction products were further analyzed by size-exclusion chromatography. These data

indicated that the mineralized protein eluted with the same retention time as the unmineralized apoferritin (Figure 2). This confirms that the overall particle size of these composite materials remains unaltered, with the mineral entrapped within the protein cage interior. No colloidal material is detected exterior to the protein cage architecture.

The products of the mineralization reactions were further characterized by transmission electron microscopy (TEM). Unstained samples showed electron dense cores of a size consistent with the interior diameter of the protein cage (Figure 3, left panel). The particle size distributions were found to be monodispersed with an average diameter of  $5.7 \pm 1$  nm. When samples were negatively stained with uranyl acetate, the intact protein cage was clearly visible as a white “halo” surrounding the metal oxide cores on the interior surface (Figure 3, right panel). Electron diffraction was not observed, suggesting that the nanoparticles generated were amorphous or poorly crystalline.

This work highlights two important concepts. First, this photochemical method allowed for the size-constrained synthesis of previously unattainable oxyhydroxide nanomaterials (Eu and Ti) using high-oxidation-state transition-metal precursors. Second, the synthetic method is general enough to be applicable to a wide variety of transition-metal/rare-earth oxyhydroxides, which could be precursors to other oxide materials.

**Acknowledgment.** This research was supported in part by grants from the National Science Foundation (Grants 0103509 and NIRT-DMR0210915), the Office of Naval Research (Grants 19-00-R006 and N00014-03-1-0692), and the National Institutes of Health (Grant 1R21EB005364).

**Supporting Information Available:** Details on the photoreduction setup, gel electrophoresis, and dynamic light scattering. This material is available free of charge via the Internet at <http://pubs.acs.org>.

IC701740Q